Requirement for nickel of the transmembrane translocation of NiFe-hydrogenase 2 in *Escherichia coli*

A. Rodrigue[a], D.H. Boxer[b], M.A. Mandrand-Berthelot[a], L.-F. Wu[a,*]

[a]*Laboratoire de Génétique Moléculaire des Microorganismes et des Interactions Cellulaires, UMR CNRS 5577, Bât. 406, INSA, 20 av. A. Einstein, 69621 Villeurbanne cedex, France*
[b]*Department of Biochemistry, Medical Sciences Institute, Dundee University, Dundee DD1 4HN, UK*

Received 19 April 1996; revised version received 8 July 1996

Abstract The cellular location of membrane-bound NiFe-hydrogenase 2 (HYD2) from *Escherichia coli* was studied by immunoblot analysis and by activity staining. Treatment of spheroplasts with trypsin was able to release active HYD2 into the soluble fraction, indicating that HYD2 is attached to the periplasmic side of the cytoplasmic membrane and that HYD2 undergoes a trans-membrane translocation during its biosynthesis. By using a *nik* mutant deficient in the high affinity specific nickel transport system, we show that the intracellular availability of nickel is essential for the processing of the large subunit and for the transmembrane translocation of HYD2. We also demonstrate that the processing of the precursor, which is related with nickel incorporation, can occur in the membrane-depleted soluble fraction and that it is associated with the increase in resistance to proteolysis of the processed form of the large subunit. The mechanism of the transmembrane translocation of HYD2 is discussed.

Key words: Nickel; Hydrogenase; *Escherichia coli*; Cellular location; Transmembrane translocation; Protein processing; Metallo-enzyme

1. Introduction

The enterobacterium *Escherichia coli* synthesizes three NiFe-hydrogenase isoenzymes (EC 1.12.-.-) under anaerobic conditions [1]. Hydrogenases 1 and 2 (HYD1 and HYD2) catalyze the anaerobic oxidation of hydrogen linked to the ultimate reduction of a terminal electron acceptor, which enables the bacterium to use hydrogen as an energy source to grow on nonfermentable carbon sources in the presence of hydrogen. It has been proposed that HYD2 catalyzes the energy-conserving oxidation of hydrogen via fumarate-reductase, whereas HYD1 is involved in the recycling of hydrogen produced by hydrogenase 3 (HYD3) [1]. HYD3 is part of the formate hydrogenlyase complex and is responsible for formate-dependent dihydrogen evolution. This system catalyzes the oxidation of endogenously produced formate to carbon dioxide and passes the electrons so generated to protons to evolve gaseous hydrogen. The overall reaction is scalar, non-energy conserving, and functions both to remove redox equivalents exchangeable with formate and to help offset acidification of the growth medium during fermentative growth. The structural genes of the three hydrogenases lie in three operons *hya, hyb* and *hyc*, each of which contains 4, 5 and 7 additional accessory genes specifically required for HYD1, HYD2 and HYD3 activities, respectively [2–5]. All three hydrogenases contain nickel [1,6–8].

Almost all NiFe-hydrogenases consist of a large subunit and a small subunit of about 60 and 30 kDa, respectively [9]. Two forms of the large subunits of NiFe-hydrogenases from several bacteria have been observed on sodium dodecyl sulfate-polyacrylamide gel electrophoresis (SDS-PAGE). The small, faster migrating form is recognized as mature form while the large, slower migrating form is considered as its precursor. The processing of the large subunits of the hydrogenase from *Azotobacter vinelandii* [10], of HYD3 from *E. coli* [8], and of the periplasmic hydrogenase from *Desulfovibrio gigas* [11] results from a proteolytic cleavage after a histidine or an arginine residue in the conserved motif Asp-Pro-Cys-Xaa-Xaa-Cys-Xaa-Xaa-His/Arg (DPCxxCxxH/R) located at the C-termini of the large subunits. The highly conserved histidyl residue is naturally substituted by an arginine in the HYD3 of *E. coli* [8]. In the purified coenzyme-F420 non-reducing selenium-containing NiFe-hydrogenase from *Methanococcus voltae*, this conserved motif is located on a third subunit composed of 25 residues. The corresponding *vhuU* gene encodes a precursor of 44 amino acids whose C-terminal part is removed after the histidyl residue during the processing [12]. The structural data indicate that the two conserved cysteines in the motif DPCxxCxxH in the large subunits of *D. gigas* provide the ligands required for the binding of nickel [11]. The processing of the large subunit of HYD3 is correlated with the nickel incorporation into the polypeptide chain [8]. The C-terminal extension in the precursor form of the large subunit of HYD3 has recently been shown to keep the protein in a conformation required for the liganding of the metal [13].

All three NiFe-hydrogenase isoenzymes of *E. coli* have been purified [6–8]. The large subunit of HYD3 is a peripheral membrane protein and is released into the soluble state when cells are broken by passage through a French press [4]. In contrast, HYD1 and HYD2 are integral membrane proteins [6,7]. HYD2 is particular in that an active HYD2 can be solubilized following treatment of the isolated membrane fraction with trypsin [14]. However, it remained unclear to which surface of the cytoplasmic membrane HYD2 is attached. In addition, the relationship between nickel insertion and membrane-targeting of the membrane-bound hydrogenases has so far remained elusive. In this communication, we report on the cellular location of HYD2 and the requirement for nickel of its trans-membrane translocation.

2. Materials and methods

2.1. Bacterial strains

HYD723 (*nikA*::MudI(*lacZ*, Amp^R)) and HYD 720 (Δ*nikA*), deriv-

*Corresponding author. Laboratoire de Chimie Bactérienne, UPR9043 CNRS, 31 chemin Joseph Aiguier, 13402 Marseille cedex 20, France. Fax: (33) 91 71 89 14. E-mail: wu@ibsm.cnrs-mrs.fr

PII S0014-5793(96)00788-0

atives of MC4100 (F^-, *araD139*, *Δ(argF-lac)*U169, *ptsF25*, *relA1*, *flbB5301*, *rpsL150*, *deoC1*, *rbsR*, λ^-), are defective in the specific nickel transport system and therefore display a hydrogenase minus phenotype [15–17]. Addition of 300 μM $NiCl_2$ to the growth medium results in restoration of the intracellular nickel concentration and hydrogenase activity in this mutant. Deletion mutant HDK203 (*Δhyb*, *Δhyc*), a derivative of MC4100, is described in [18].

2.2. Media and growth conditions

Bacteria were routinely grown in LB medium or on LB plates [19]. Anaerobic growth was achieved normally in LB medium supplemented with 2 μM sodium selenite and 2 μM ammonium molybdate in 100-ml bottles filled to the top or on LB plates in GasPak anaerobic jars (BBL Microbiology Systems). When required, ampicillin (50 μg/ml) and kanamycin (20 μg/ml) were added. To assess the influence of nickel on HYD2 synthesis, 300 μM $NiCl_2$ was added to the growth medium when noted.

2.3. Activity staining

To detect HYD1 and HYD2 activities specifically, crude extracts were separated on 7.5% non-denaturing polyacrylamide gels and HYD1 and HYD2 were visualized with a benzyl viologen-linked hydrogen uptake assay [14]. The activity bands were fixed by the addition of 1 mM 2,3,5-triphenyltetrazolium chloride. Protein concentration was determined by using the DC Protein assay kit (BioRad).

2.4. Western blot analysis

Denatured polypeptides were separated by sodium dodecyl sulfate-polyacrylamide gel (7.5%) electrophoresis (SDS-PAGE) [20]. Immunoblotting was performed by using the ECL method according to the manufacturer's (Amersham) instruction. Antisera were used at the following dilution: anti-HYD1 1/20000, anti-HYD2 1/10000, and goat anti-rabbit IgG-peroxidase 1/20000.

2.5. Preparation of spheroplasts, and membrane fraction

Anaerobic grown bacteria were sedimented from exponential cultures (A_{600} = 0.5) by centrifugation at 7000×*g* for 15 min at 4°C. Cells were broken by 2 passages through a French press cell. Crude extracts were obtained by centrifugation at 20000×*g* for 15 min. The membrane and soluble fractions were prepared by further centrifugation of the supernatant at 130000×*g* for 2 h at 4°C. The membrane pellets were resuspended in 50 mM Tris-HCl (pH 7.0) supplemented with 6 M urea, and then ultracentrifuged under the same conditions. The pellets were washed twice with 50 mM Tris-HCl (pH 7.0) and resuspended to a protein concentration of 0.3 mg/ml in the same buffer. The soluble fraction was obtained by centrifugation for 2 h at 130000×*g* the supernatant from the first ultracentrifugation. Spheroplasts were prepared from whole bacterial cells by a lysozyme/EDTA method [21] and the periplasmic fraction was separated from the spheroplasts by centrifugation at 5000×*g* for 10 min. The resulting spheroplasts were washed once and resuspended to a protein concentration of 25 mg/ml in the Tris-HCl buffer and then treated by trypsin at 0.25 mg/ml for 60 min at 30°C. The reaction was stopped by adding into the reaction solution the protease inhibitor Pefabloc (Boehringer Mannheim) at a final concentration of 1 mM and the solubilized proteins were separated from the spheroplasts by centrifugation at 15000×*g* for 10 min.

2.6. Monitoring conformational change by limited proteolysis

The conformational change of the precursor of the large subunit of HYD2 was monitored by limited proteolysis. The *nik* mutant HYD720 was grown anaerobically until the logarithmic growth phase (OD_{600}=0.4) in 2 l LB medium in the absence of nickel. Cells were harvested, washed with phosphate buffer (50 mM Na_2HPO_4, 50 mM KH_2PO_4, pH 6.8), resuspended into 40 ml of the same phosphate buffer with 0.5 mM β-mercaptoethanol and broken by 2 passages through a French press. The cell debris was eliminated by centrifugation at 15000×*g* for 15 min and the supernatant was saved as a crude extract. To obtain a soluble fraction free of membrane, the crude extract was centrifuged twice each for 90 min at 220000×*g*. To initiate the processing of the precursor (HybC-P), 500 μM $NiCl_2$ was added to the soluble fraction and incubated at 30°C for 3 h. The reaction mixture was aliquoted and proteinase K was added at final concentrations of 0, 1, 2, 5 and 8 μg/ml. After 20 min incubation at room temperature, proteolysis was stopped by adding 1 mM Pefabloc. The samples were precipitated with 5% trichloroacetic acid, resolved by SDS-PAGE, and the precursor (HybC-P) and the processed form (HybC-M) of the large subunit of HYD2 were analyzed by immunoblotting.

3. Results

3.1. Effects of nickel on the processing of the precursor of the large subunit (HybC) of HYD2 and its membrane targeting

We previously reported that the *nik* (*hydC*) mutant is defective in the specific nickel transport system and that its intracellular nickel concentration is less than 1% of the level of a wild-type strain, which results in the absence of hydrogenase activity (HYD^- phenotype). The addition of nickel to the growth medium specifically restores the intracellular nickel concentration and the hydrogenase activity in this mutant [15–17]. In this case, nickel is taken up through the nonspecific magnesium transport system. In the absence of nickel neither HYD1 nor HYD2 can be detected immunologically in the membrane fraction of the *nik* mutant [16], which suggests that the lack of a functional *nik* product either abolishes the expression of hydrogenases or prevents the hydrogenase precursors from being targeted to the membrane. To assess this point we examined the biosynthesis of the hydrogenases and their cellular location by immunoblotting.

Three polypeptides were detected in the crude extracts of the wild-type strain (Fig. 1, lane 1), using antiserum against the large subunit (HybC) of HYD2. The polypeptide with the highest molecular weight (approx. 65000) must be a contaminating band detected that is not related to HYD2 since it was also present in the crude extract of the *hyb* deletion mutant (Fig. 1, lane 10). The two specific bands with apparent molecular weights of 62500 and 61000 correspond to the sizes predicted from the *hybC* gene sequence for the precursor (HybC-P) and the processed (HybC-M) form of the large subunit of HYD2, respectively. The processed form was detected in both the soluble (Fig. 1, lane 2) and membrane (Fig. 1, lane 3) fractions, whereas the precursor was present exclusively in the soluble fraction. Immunoblot analysis revealed the presence of the precursor in the crude extract of the *nik* mutant cells grown without nickel (Fig. 1, lane 4). Therefore, HYD2

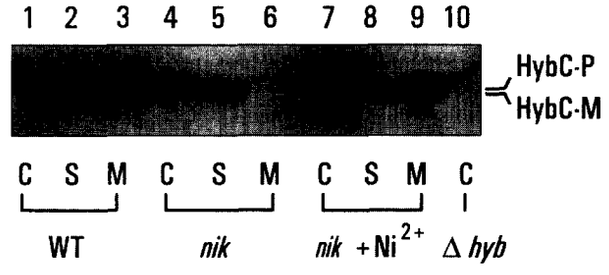

Fig. 1. Intracellular nickel availability is essential for the processing and membrane targeting of the large subunit of HYD2. After anaerobic growth the following strains were tested: the wild-type strain MC4100 (lanes 1–3); the *nik* mutant HYD723 deficient in specific nickel transport system, grown without (lanes 4–6) or with 300 μM $NiCl_2$ (lanes 7–9) and the *hyb* deletion mutant HDK203 (lane 10). About 20 μg proteins from crude extracts (C), or soluble (S) fractions, or 30 μg proteins from the membrane (M) fractions were subjected to SDS-PAGE (7.5%) electrophoresis and analyzed by immunoblot analysis employing antisera raised against the large subunit of HYD2, HybC. The precursor (HybC-P) and the processed (HybC-M) forms of HybC are indicated on the right.

is in fact synthesized in the *nik* mutant in the absence of nickel, but it accumulates in the precursor form (HybC-P). In addition, this precursor form (HybC-P) was present exclusively in the soluble fraction (Fig. 1, lane 5), and absent from the membrane fraction (Fig. 1, lane 6) under this condition. The addition of nickel to the growth medium resulted in the appearance of the smaller processed form of HybC (HybC-M), which became detectable in both the soluble and membrane fractions (Fig. 1, lanes 7–9). The pattern of HybC processing and subcellular distribution in the *nik* mutant complemented with nickel was similar to that of the wild-type parental strain (Fig. 1, compare lanes 1–3 with lanes 7–9). These results are consistent with our previous observation that HYD2 is absent from the membrane fraction in the *nik* mutant grown without nickel [16]. In addition, they indicate that the lack of a functional *nik* product prevents the hydrogenase precursor from being processed and targeted to the membrane. Since the large subunit was not detectable in the periplasmic fraction (see below in Fig. 2), the precursor HybC-P must accumulate in the cytoplasmic fraction. Furthermore, this result suggests that the processing of the large subunit (HybC) of HYD2 occurs in the cytoplasm. Identical results were obtained with respect to HYD1 processing and membrane targeting (data not shown). Therefore, intracellular availability of nickel is a prerequisite required for HYD2, as well as for HYD1, processing and membrane targeting.

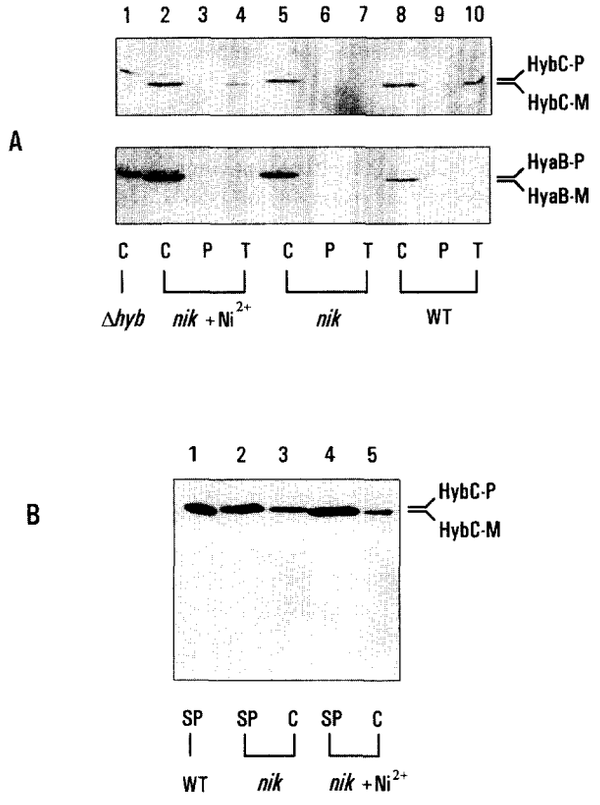

Fig. 2. Cellular localization of the large subunits of HYD1 and HYD2. Antisera raised against the large subunit of HYD2 (HybC, A, upper panel; B), or the large subunit of HYD1 (HyaB, A, lower panel) were used to analyze, in panel A, crude extracts (C), periplasmic fractions (P), or the trypsin-solubilized fractions (T) obtained after the exposure of spheroplasts to trypsin. Shown are results obtained with wild-type strain MC4100 (WT), *hyb* deletion mutant HDK203 (Δ*hyb*) and *nik* mutant HYD723 (*nikA*::MudI) grown anaerobically in the absence (*nik*) or presence (*nik*+Ni^{2+}) of 300 μM $NiCl_2$. After immunoblotting using anti-HybC antiserum (upper panel), the polyvinylidene difluoride (PVDF) membrane was stripped of bound antibodies and reprobed with anti-HyaB antiserum (lower panel). (B) To analyze whether the cytoplasmic membrane remains intact after trypsin treatment, the spheroplasts (lanes 1,2,4) obtained from the same cells as described in A and the same crude extracts (lanes 3,5) as those in A, lanes 5 and 2, were resolved by SDS-PAGE, and the precursor (HybC-P) and the processed form (HybC-M) of the large subunit of HYD2 were analyzed by immunoblotting.

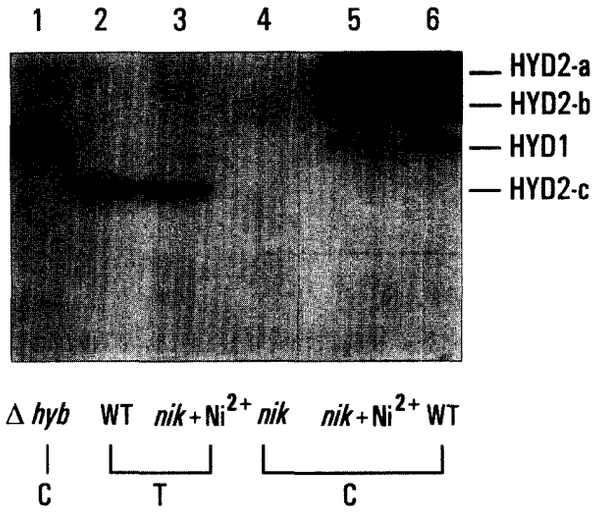

Fig. 3. Release of active HYD2 from spheroplasts by trypsin proteolysis. The same samples as those in Fig. 2 were electrophoresed on native polyacrylamide gel (7.5% w/v) and subjected to hydrogenase activity staining as described in Section 2. HYD1 and the three forms of HYD2 are indicated on the right.

3.2. Periplasmic side location of HYD2

In an early investigation using membrane-impermeant probes, Graham reported that a membrane-bound hydrogenase (Mol. Wt approx. 63 000) is accessible from both sides of the cytoplasmic membrane [22]. Sauter et al. showed that the large subunit of HYD3 (61 000) is a peripheral membrane protein being released into the soluble state when cells are broken by passage through a French Press [4]. In addition, an active soluble HYD2 consisting of both large (61 000) and small (30 000) subunits was released from the membrane fraction by trypsin treatment [7]. Compared to this trypsin released derivative of HYD2, the detergent-dispersed native HYD2 is composed of the identical large subunit, but its small subunit is some 5 kDa larger than this subunit in the trypsin-treated enzyme [7]. Trypsin, therefore, cleaves the small subunit of HYD2. This cleavage correlates with the release of the active fragment from the membrane. However, it has not been established on which surface of the membrane the HYD2 is attached. These results illustrate a complex organization of the various hydrogenases in the membrane.

We investigated the orientation of HYD2 within the cytoplasmic membrane by immunoblotting and by activity staining. The large subunit (HybC) of HYD2 was detected in the crude extract (C) but was absent from the periplasmic fraction (P) in a wild-type strain (Fig. 2A, lanes 8,9). Limited tryptic proteolysis of the spheroplasts released HybC into the soluble fraction (Fig. 2A, lane 10), indicating that HybC is accessible

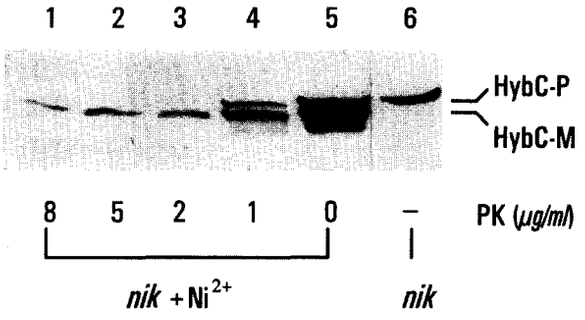

Fig. 4. Conformational change of the large subunit of HYD2 as defined by sensitivity to proteolysis. In vitro processing of the precursor of the large subunit of HYD2 from the *nik* mutant HYD720 grown anaerobically in the absence of nickel was performed by adding 500 μM $NiCl_2$ to the membrane-depleted soluble fraction as described in Section 2. The reaction mixture containing equal amounts of the precursor (HybC-P) and the processed form (HybC-M) of the large subunit of HYD2 was aliquoted and subjected to proteolysis in the presence of 0, 1, 2, 5, and 8 μg/ml proteinase K (PK, as indicated) at room temperature for 20 min. Proteolysis was stopped by 1 mM Pefabloc. The samples were precipitated with 5% trichloroacetic acid, resolved by SDS-PAGE, and the precursor (HybC-P) and the processed form (HybC-M) of the large subunit of HYD2 were analyzed by immunoblotting. Lane 6 shows the precursor of the large subunit of HYD2 present in the membrane-depleted soluble fraction before the processing procedure.

from the periplasmic surface of the cytoplasmic membrane. To ensure that the trypsin solubilized fraction (T) is not contaminated by the membrane, the polyvinylidene difluoride (PVDF) blotting membrane was stripped of bound antibodies and reprobed with anti-HyaB antiserum against the large subunit (HyaB) of HYD1 to check the location of HyaB. The previous finding that HYD1 cannot be released from the membrane by trypsin treatment [6] implies that it is transmembranous or that the trypsin-cutting sites of HYD1 are poorly accessible. The absence of the large subunit HyaB of HYD1 from the trypsin solubilized fractions (T) is consistent with the previous report [6] and thus confirms that the trypsin-solubilized fractions were appropriately prepared (Fig. 2A, lane 10). In the *nik* mutant grown in the absence of nickel, only the precursor HybC-P was found in the crude extracts and it was undetectable in the periplasmic fraction nor was it released by trypsin treatment from the spheroplasts (Fig. 2A, lanes 5–7). Addition of nickel to the growth medium confers the wild-type patterns of the cellular location and processing of HybC on the *nik* mutant (Fig. 2A, lanes 2–4).

In addition, examination of spheroplasts after incubation with trypsin did not reveal any accumulation of proteolysed form of the large subunit (HybC) of HYD2 (Fig. 2B, lanes 1,2,4). This suggests that the cytoplasmic membrane remains intact and that cleavage of the small subunit is itself sufficient for release of HYD2 from the membrane.

In accordance with the results obtained by immunoblotting, hydrogenase activity staining confirms the accessibility of HYD2 in the spheroplasts. Crude extracts of different cells or trypsin-released soluble fractions of the spheroplasts were separated by native PAGE and hydrogenase enzymes were visualized by activity staining. Wild-type strain MC4100 exhibited three active bands (Fig. 3, lane 6), which is in good agreement with the result previously reported by Sawers and Boxer [6]. As they demonstrated, the faster migrating band corresponds to HYD1 while the two more slowly migrating bands are HYD2. The difference between the two forms of HYD2 is unknown. As anticipated, mutant HDK203 carrying a deletion in the *hyb* operon displays only HYD1 activity (Fig. 3, lane 1). In this experiment, the HYD1 was a slow developing band. Thus, when it is appropriately visualized the two HYD2 bands (HYD2-a and HYD2-b) are over-developed and form an active zone, instead of two distinguishable bands. As expected the *nik* mutant grown without nickel did not contain any hydrogenase activity (Fig. 3, lane 4), whereas it showed a similar profile to the wild-type strain when nickel was added in the growth medium (Fig. 3, lane 5). Exposure to trypsin of spheroplasts prepared from a wild-type strain or the *nik* mutant grown with nickel released the active HYD2 into the supernatant (T) (Fig. 3, lanes 2,3; HYD2-c). The released HYD2 showed faster mobility than HYD1. Consistently, an increase in electrophoretic mobility of HYD2 after release from the membrane fraction by proteolytic treatment was reported by Ballantine and Boxer [7]. The increase in mobility may result from cleavage of the 5 kDa fragment of the small subunit in the solubilized HYD2 complex.

3.3. *Conformational difference between the cytoplasmic precursor HybC-P and its processed form HybC-M*

Addition of nickel to the growth medium leads to the processing of the precursor (HybC-P) of HYD2. The incorporation of nickel into the precursor followed by its processing must be associated with a conformational change. Sensitivity to proteolytic degradation was used to monitor conformational change of the precursor upon the incorporation of nickel and its processing in vitro. A membrane-depleted soluble fraction was prepared from the *nik* mutant HYD720 grown anaerobically in the absence of nickel. To initiate the processing of the precursor (HybC-P), 500 μM $NiCl_2$ was added to the in vitro processing medium. 3 h later, proteinase K was added at various final concentrations. After 20 min incubation with proteinase K, proteolysis was stopped by adding the protease inhibitor Pefabloc and the content of the precursor (HybC-P) and the processed form (HybC-M) of the large subunit of HYD2 was analyzed by immunoblotting. As expected, only the precursor form (HybC-P) was revealed in the absence of nickel (Fig. 4, lane 6). About 50% precursor was converted to the processed form (HybC-M) after 3 h of incubation with 500 μM $NiCl_2$ (lane 5), which indicates that the processing of the precursor is independent on the presence of the cytoplasmic membrane. A polypeptide with a lower molecular weight than the processed form of HybC was also detected by the anti-HybC antiserum in the absence of proteinase K (lane 5). This band may result from the proteolysis of the HybC-P or/and HybC-M by an endogenous protease, since no protease inhibitor was added to the reaction medium. The amount of the precursor (HybC-P) was reduced to about 30% that of the processed form (HybC-M) after 20 min treatment with 1 μg/ml proteinase K. The precursor was completely digested by 2 μg/ml proteinase K (lane 3), whereas the processed form was resistant to proteolysis at a concentration of proteinase K up to 8 μg/ml (lane 1). Thus incorporation of nickel and processing of the precursor lead to a conformation change, and the residues of the processed form HybC-M are associated in higher order structures that render the peptide bonds less accessible to protease than those in the precursor HybC-P.

4. Discussion

Biosynthesis of the NiFe-hydrogenase metalloenzymes is a complex process. It involves the incorporation of nickel into hydrogenase apoprotein, assembly of the holoenzymes, translocation across the cytoplasmic membrane and processing of the small and large subunits. It is still unknown in which order these processes take place and whether further reactions are required. It has been shown that nickel insertion into the precursors is a prerequisite for the large subunit C-terminal processing of the hydrogenase of *A. vinelandii* [23], HYD1 [24] and HYD3 of *E. coli* [25]. In this communication, we show that the intracellular availability of nickel is essential for HYD2 translocation to the periplasmic side of the membrane.

The mechanism of nickel incorporation involves a number of steps which are subjected to current investigation. The gene products of the *hyp* operon are required for the maturation of catalytically active hydrogenases [18]. Among them, the HypB protein exhibiting a low intrinsic GTPase activity is directly involved in nickel insertion into the precursor of the large subunit of HYD3 and its processing [25,26]. Proteins homologous to HypB are also found in *Rhodobacter capsulatus, Rhizobium leguminosarum, A. vinelandii* and *Alcaligenes eutrophus* (for a review, see [27]).

We recently investigated the involvement of the chaperonins GroEL and GroES in the biosynthesis of the hydrogenase isoenzymes in *E. coli* [28]. Lesions in *groEL* and *groES* severely affect HYD3 activity and processing of its large subunit while they have only a marginal effect on HYD2. In addition, chaperonins were proposed to assist the precursor form of the large subunit of HYD3 to reach a conformation competent for the insertion of nickel. Therefore, apart from accessory gene products like HypB which display a function of incorporation common to all three hydrogenase isoenzymes, specific chaperonin proteins may be involved in the biosynthesis of the nickel center of these related enzymes.

The crystal structure of the NiFe-hydrogenase from *D. gigas* has recently revealed that the active site containing nickel and a second metal ion, probably an iron, is deeply buried in the 60 kDa large subunit [11]. The lack of the last 15 C-terminal residues deduced from gene sequence indicates that cleavage occurs next the DPCxxCxxH motif just after the histidyl residue conserved in almost all nickel-containing hydrogenases. Removal of the corresponding C-terminal peptide from the large subunit of HYD3 is catalysed by the specific HycI protease once nickel is inserted into the precursor [5,8]. In order to provide easy access for nickel or the nickel-carrier protein, the DPCxxCxxH motif harboring the two cysteinyl residues which serve as bridging ligands for nickel in the active center, and the extra C-terminal segment are assumably located at the surface of the precursor of the large subunit. This C-terminal extension in the precursor form of the large subunit of HYD3 has been demonstrated to have a function in keeping the protein in a conformation necessary for the coordination of the metal [13]. Incorporation of nickel into the active center might trigger a conformational change accompanied with the removal of the C-terminal extension, which will result in the burial of the active site in the mature enzyme. Removal of the C-terminal peptide will render these processes irreversible. Our results show that incorporation of nickel into the precursor followed by its processing results in a significant conformational change of the large subunit of HYD2. The increasing resistance to proteolysis of the processed form HybC-M implies that the large subunit attains a stably folded conformation upon incorporation of nickel and removal of the extra C-terminal segment (Fig. 4).

Three observations suggest that incorporation of nickel into the precursor and its processing are achieved in the cytoplasm. First, intracellular nickel availability is essential for membrane targeting and processing of HYD2, which is attached to the periplasmic side of the cytoplasmic membrane (Fig. 1). Second, the processed form of HYD2 was detected both in the cytoplasm and in the membrane, while its precursor was found exclusively in the cytoplasm (Fig. 1). Finally, nickel-dependent processing of the precursor can occur in the membrane-depleted soluble fraction (Fig. 4). It is not known, however, how the stably folded large subunit of HYD2 crosses the cytoplasmic membrane.

Alternative pathways have been described for the formation of a metallo-center and the translocation of the corresponding metallo-enzymes. Masui et al. [29] reported that spheroplasts from a molybdenum cofactor-deficient mutant of *Rhodobacter sphaeroides* f. sp. *denitrificans* is capable of secreting the dimethyl sulfoxide (DMSO) reductase apoprotein into the periplasm. This indicates that translocation of the DMSO reductase is independent on the incorporation of the molybdenum cofactor. More recently, the DipZ membrane-bound protein has been described as essential for maintaining cytochrome *c* apoproteins in the correct conformations for the covalent attachment of haem groups to the appropriate pairs of cysteine residues [30]. Therefore, incorporation of the haem groups seems to be associated with the translocation and to occur in the membrane.

Particularity of hydrogenase translocation resides in the possible cotranslocation of the small and the large subunits. The fact that only the small subunits contain the N-terminal signal sequence suggests that the formation of a complex composed of precursors of the small and the large subunits is a prerequisite for hydrogenase translocation [9,31,32]. However, the relationship among nickel incorporation, large subunit processing and formation of the complex remains to be established. We recently observed that expression of the large subunit of HYD2 in the absence of the small subunit resulted in the accumulation of the large subunit in the precursor form (A. Rodrigue, unpublished data). This suggests that processing of the large subunit is dependent on the small subunit and that formation of the complex is a prerequisite for the large subunit processing. Our future studies will focus on characterization of formation of the HYD2 complex and its transmembrane translocation.

Acknowledgements: We acknowledge A. Böck for strain HDK203. This work was supported by grant from the Centre National de la Recherche Scientifique to UMR CNRS 5577 and by Procope program no. 95068.

References

[1] Sawers, R.G., Ballantine, S.P. and Boxer, D.H. (1985) J. Bacteriol. 164, 1324–1331.
[2] Menon, N.K., Robbins, J., Peck, Jr., H.D.P., Chatelus, C.Y., Choi, E.S. and Przybyla, A.E. (1990) J. Bacteriol. 172, 1969–1977.
[3] Menon, N.K., Chatelus, C.Y., Dervartanian, M., Wendt, J., Shanmugam, K.T., Peck Jr., H.D.P. and Przybyla, A.E. (1994) J. Bacteriol. 176, 4416–4423.

[4] Sauter, M., Böhm, R. and Böck, A. (1992) Mol. Microbiol. 6, 1523–1532.
[5] Rossmann, R., Maier, T., Lottspeich, F. and Böck, A. (1995) Eur. J. Biochem. 227, 545–550.
[6] Sawers, R.G. and Boxer, D.H. (1986) Eur. J. Biochem. 156, 265–275.
[7] Ballantine, S.P. and Boxer, D.H. (1986) Eur. J. Biochem. 156, 277–284.
[8] Rossmann, R., Sauter, M., Lottspeich, F. and Böck, A. (1994) Eur. J. Biochem. 220, 377–384.
[9] Wu, L.-F. and Mandrand, M.A. (1993) FEMS Microbiol. Rev. 104, 243–270.
[10] Gollin, D.J., Mortenson, L.E. and Robson, R.L. (1992) FEBS Lett. 309, 371–375.
[11] Volbeda, A., Charon, M.-H., Piras, C., Hatchikian, E.C., Frey, M. and Fontecilla-Camps, J.C. (1995) Nature 373, 580–587.
[12] Sorgenfrei, O., Linder, D., Karas, M. and Klein, A. (1993) Eur. J. Biochem. 213, 1355–1358.
[13] Binder, U., Maier, T. and Böck, A. (1996) Arch. Microbiol. 165, 69–72.
[14] Ballantine, S.P. and Boxer, D.H. (1985) J. Bacteriol. 163, 454–459.
[15] Wu, L.-F. and Mandrand-Berthelot, M.A. (1986) Biochimie 68, 167–179.
[16] Wu, L.-F., Mandrand-Berthelot, M.A., Waugh, R., Edmont, C.J., Holt, S.E. and Boxer, D.H. (1989) Mol. Microbiol. 3, 1709–1718.
[17] Navarro, C., Wu, L.-F. and Mandrand-Berthelot, M.A. (1993) Mol. Microbiol. 9, 1181–1191.
[18] Jacobi, A., Rossmann, R. and Böck, A. (1992) Arch. Microbiol. 158, 444–451.
[19] Miller, J.H. (1972) Experiments in Molecular Genetics, Cold Spring Harbor Laboratory, Cold Spring Harbor, NY.
[20] Laemmli, U.K. (1970) Nature 277, 680–685.
[21] Osborn, M.J., Gander, J.E. and Parisi, E. (1972) J. Biol. Chem. 247, 3973–3986.
[22] Graham, A. (1981) Biochem. J. 197, 283–291.
[23] Menon, A.L. and Robson, R.L. (1994) J. Bacteriol. 176, 291–295.
[24] Menon, N.K., Robbins, J., Wendt, J.C., Shanmugam, K.T. and Przybyla, A.E. (1991) J. Bacteriol. 173, 4851–4861.
[25] Maier, T., Jacobi, A., Sauter, M. and Böck, A. (1993) J. Bacteriol. 175, 630–635.
[26] Maier, T., Lottspeich, F. and Böck, A. (1995) Eur. J. Biochem. 203, 133–138.
[27] Vignais, P.M. and Toussaint, B. (1994) Arch. Microbiol. 161, 1–10.
[28] Rodrigue, A., Batia, N., Müller, M., Fayet, O., Böhm, R., Mandrand-Berthelot, M.A. and Wu, L.-F. (1996) J. Bacteriol. 178, in press.
[29] Masui, H., Satoh, M. and Satoh, T. (1994) J. Bacteriol. 176, 1624–1629.
[30] Crooke, H. and Cole, J. (1995) Mol. Microbiol. 15, 1139–1150.
[31] Nivière, V., Wong, S.L. and Voordouw, G. (1992) J. Gen. Microbiol. 138, 2173–2183.
[32] Voordouw, G. (1992) Adv. Inorg. Chem. 38, 397–422.